

Multi-physics code system with improved feedback modeling



Mine O. Yilmaz ^a, Maria N. Avramova ^{b,*}, Jens G.M. Andersen ^c

^a Department of Mechanical and Nuclear Engineering, The Pennsylvania State University, University Park, PA, 16802, United States

^b Department of Nuclear Engineering, North Carolina State University, Raleigh, NC 27695, United States

^c Retired Thermal-Hydraulics Chief Consulting Engineer, GE-Hitachi Nuclear Energy, United States

ARTICLE INFO

Article history:

Received 2 April 2016

Received in revised form

10 July 2016

Accepted 2 March 2017

Available online 9 March 2017

Keywords:

Doppler feedback

Fuel thermal conductivity degradation

Nuclear reactor multi-physics

CTF/TORT-TD

CTF/TORT-TD/FRAPCON-FRAPTRAN

ABSTRACT

Fuel temperature (Doppler) feedback modeling in the coupled sub-channel thermal-hydraulic/time dependent neutron transport codes system CTF/TORT-TD was improved by accounting for the burnup dependence of the fuel thermal conductivity. TORT-TD is a three-dimensional (3D) time dependent neutron-kinetics code based on the discrete ordinates (S_N) method. CTF is the Reactor Dynamics and Fuel Modeling Group (RDFMG) version of the sub-channel thermal-hydraulics code COBRA-TF (COLant Boiling in Rod Arrays – Two Fluid). A burnup-dependent fuel rod model, which takes into account the degradation of the fuel thermal conductivity at high burnups and the effects of burnable poisons, such as Gadolinium, was implemented in CTF. The model is applicable to UO₂ (uranium dioxide) and MOX (mixed oxide) nuclear fuels – it includes the modified Nuclear Fuel Industries (NFI) model for UO₂ fuels and the Duriez/Modified NFI model for MOX fuels. The in-pellet fuel temperature distributions predicted by CTF/TORT-TD were compared to reference CTF/TORT-TD/FRAPCON calculations, in which the fuel rods were modeled with the fuel performance code FRAPCON. These comparisons were carried out for a 4 × 4 pressurized water reactor (PWR) pin array at hot full power (HFP) steady state conditions. The CTF/TORT-TD fuel temperature predictions were consistent with the CTF/TORT-TD/FRAPCON results. This fact demonstrated that CTF with the new fuel thermal conductivity model can predict the temperature field within light water reactor (LWR) fuel rods as accurately as FRAPCON. Therefore, CTF/TORT-TD calculations can be carried out in fast scoping studies instead of the computationally expensive CTF/TORT-TD/FRAPCON calculations. The performed statistical analyses indicated an improved accuracy of fuel temperature calculations relative to the CTF/TORT-TD/FRAPCON reference numerical solution. Furthermore, better agreement between CTF/TORT-TD and CTF/TORT-TD/FRAPCON in calculated neutronic reactivity was found when fuel burnup effects were considered in CTF/TORT-TD. Therefore, the improved CTF/TORT-TD can be seen as a high fidelity multi-physics computational tool capable of providing accurate and efficient simulations for practical reactor core design and safety analysis.

© 2017 Elsevier Ltd. All rights reserved.

1. Introduction

Models for degradation of the fuel thermal conductivity with burnup already exist in the fuel performance codes such as FRAPCON and FRAPTRAN-3.4 (Geelhood et al., 2010a, 2010b; Lusher and Geelhood, 2010), whereas most of the thermal-hydraulics codes still use simplified fuel rod models along with the 1979 MATPRO-11 material properties of unirradiated UO₂ (uranium dioxide). Modeling of the fuel thermal conductivity degradation (TCD) is of

high importance for accurate predictions of the fuel temperature (Doppler) feedback and thus for reactor safety evaluations.

The modified Nuclear Fuel Industries (NFI) (Lusher and Geelhood, 2010) model for UO₂ fuel rods and the Duriez/Modified NFI model (Lusher and Geelhood, 2010) for MOX (mixed oxide) fuel rods were already implemented in the stand-alone CTF (Salko and Avramova, 2013). The two models take into account the degradation of the fuel thermal conductivity with high burnups and its dependence on the presence of burnable poisons such as Gadolinium, for example. The modified CTF was validated using the Halden fuel temperature measurements (Geelhood et al., 2010c). In addition, a CTF-to-FRAPCON-3.4 benchmarking was carried out (Yilmaz, 2014). It was demonstrated that overall CTF with the burnup-dependent fuel thermal conductivity models predicts the

* Corresponding author. 2500 Stinson Drive, Raleigh, NC, 27695, United States.

E-mail addresses: ozdemirmine@hotmail.com (M.O. Yilmaz), mnnavramo@ncsu.edu (M.N. Avramova), jandersen@ec.rr.com (J.G.M. Andersen).

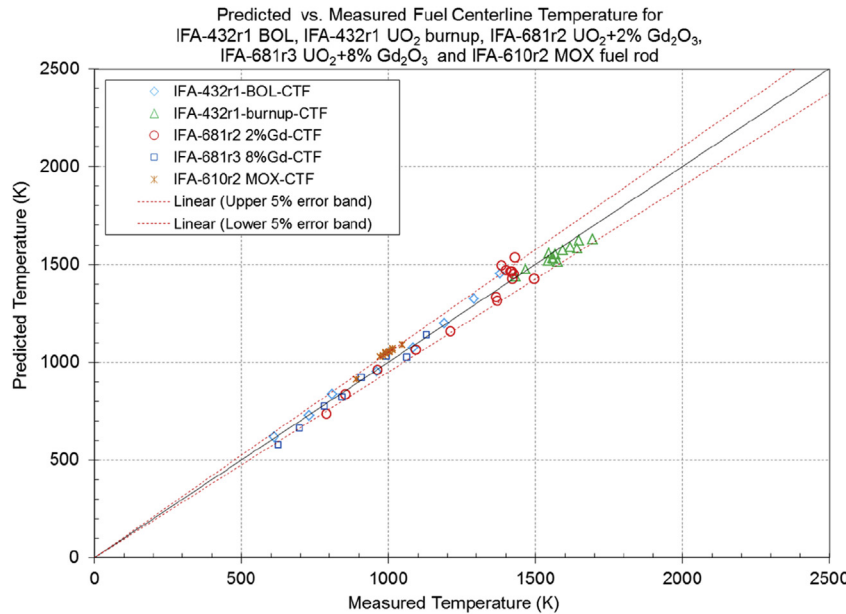


Fig. 1. Predicted vs. Measured Fuel Centerline Temperature for IFA-432r1 BOL, IFA-432r1 burnup, IFA-681r2 $\text{UO}_2 + 2\% \text{Gd}_2\text{O}_3$, 681r3 $\text{UO}_2 + 8\% \text{Gd}_2\text{O}_3$ and IFA-610r2 MOX.

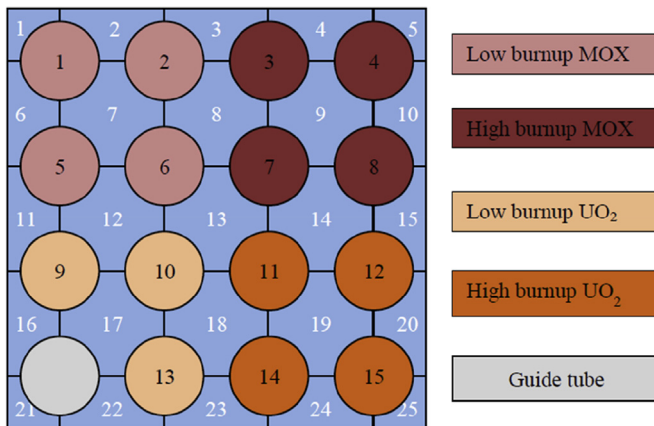


Fig. 2. 4×4 PWR Pin array and sub-channel Configuration.

Table 1
As-manufactured cold fuel dimensions.

Active length [m]	3.6576
Pin pitch [m]	0.0126
Fuel pellet radius [m]	0.003951
Inner clad radius [m]	0.004010
Outer clad radius [m]	0.004583
Clad-pellet gap thickness [m]	0.000059
Clad thickness [m]	0.000573

Halden experimental data within a 5% error band (Fig. 1).

The burnup-dependent fuel thermal conductivity model was also incorporated in the coupled sub-channel thermal-hydraulics/time-dependent neutron transport code system CTF/TORT-TD (Magedanz et al., 2015). The hot full power (HFP) steady state conditions were simulated for a 4×4 pin array (Fig. 2) extracted from the Purdue Pressurized Water Reactor (PWR) MOX benchmark (Kozlowski and Downar, 2007). The CTF/TORT-TD simulations

Table 2
Input parameters for UO_2 and MOX fuel types.

Cold plenum length [m]	0.22
Outer diameter of plenum spring [m]	0.007902
Diameter of the plenum spring wire [m]	0.001006
Number of turns in the plenum spring	20
Length of each pellet [m]	0.011003
Depth of pellet dish [m]	0.000280
Pellet dish shoulder width [m]	0.001036
Pellet surface roughness [m]	2.10^{-6}
Expected density increase during operation [kg/m^3]	100.0
Clad type	Zircaloy 4
Cladding inner surface roughness [m]	$5.0038 \cdot 10^{-7}$
Initial gas pressure [Pa]	$2.0 \cdot 10^6$
Coolant pressure [MPa]	15.5
Coolant inlet temperature [$^\circ\text{K}$]	560.0
Coolant mass flux [$\text{kg}/(\text{m}^2 \text{s})$]	3062.88
Linear power [kW/m] (axially uniform)	19.13
Time step interval size [days]	50
Burn time [days]	1000

Table 3
FRAPCON nodalization of the UO_2 and MOX rods.

Pellet radial nodes (equal cross-sectional area)	17
Axial nodes (equal length)	20

Table 4
 UO_2 and MOX fuel characteristics.

	UO_2	MOX
U-235 enrichment [%]	4.25	0.202
PuO_2 content [%]	N/A	5.0
% of theoretical density	93.35	94.67

were performed with and without modeling of the fuel TCD and the results were compared to CTF/TORT-TD/FRAPTRAN predictions (Magedanz et al., 2015). The CTF/TORT-TD/FRAPTRAN sub-channel thermal-hydraulic/time-dependent neutron transport/fuel

Table 5
Sub-channel geometry information.

Sub-channel type	Area [m ²]	Wetted perimeter [m]	Number of sub-channels
Central	0.0000928	0.0288	9
Side	0.0000464	0.0144	12
Corner	0.0000232	0.00720	4

Table 6
Inter-channel transverse connections information.

Sub-channel connection type	Length [m]	Width [m]	Horizontal loss coefficient	Number of gaps
Half gap width	0.0126	0.001717	0.5	16
Full gap width	0.0126	0.003434	0.5	24

Table 7
Modeling options used in CTF.

Rod friction model	$\lambda = 0.204Re^{-0.2}$
Entrainment/deposition	Original model
Mixing/void drift	Specify mixing coefficient
Equilibrium drift factor	1.4
2-phase turbulent mixing coefficient	0.004
Maximum time step size [s]	0.01 for steady state 0.001 during rod ejection

Table 8
Boundary conditions used in CTF.

Inlet enthalpy [kW/kg]	1267.9
Inlet mass flow [kg/s]	4.5465
Outlet pressure [MPa]	15.5

Table 9
CTF radial and axial nodalization.

Pellet radial nodes (equal mesh)	15
Cladding radial nodes	2
Axial nodes (equal length)	20

Table 10
CTF spacer grid information.

Spacer grid loss coefficient	1.701
Number of spacer grids	10 (at even-numbered nodes)

performance coupled calculations were considered reference solutions: TORT-TD provided the time-dependent neutron transport solution on a pin-by-pin homogenized level; FRAPTRAN accounted for the thermo-mechanical changes within the fuel rod (pellet-gap-cladding) during the transient; and CTF solved for the time-dependent coolant flow conditions. Please note that, although in (Magedanz et al., 2015) the coupled code system is called CTF/TORT-TD/FRAPTRAN, it uses FRAPCON-generated data for steady state calculations. In other words, the CTF/TORT-TD/FRAPCON is used to generate reference solutions for steady state conditions while the CTF/TORT-TD/FRAPTRAN does the same for transient scenarios. The agreement between CTF/TORT-TD and CTF/TORT-TD/FRAPCON predictions of the fuel temperature demonstrated that CTF with the new fuel thermal conductivity model can predict the temperature field within LWR fuel rods as accurately as FRAPCON; and therefore, CTF/TORT-TD calculations can be carried out in fast scoping studies.

2. Description of the multi-physics code systems

As previously discussed, the 4×4 fuel bundle configuration shown in Fig. 2 was used to assess the performance of the new CTF fuel thermal conductivity model for multi-rod/multi-channel configurations. The array consists of fifteen (15) PWR pins and one (1) control rod guide tube. There are four (4) types of fuel rods within the array: low burnup MOX, high burnup MOX, low burnup UO₂ and high burnup UO₂. This configuration allows testing of the fuel rod models in CTF and FRAPCON for different fuel types with different burnup levels (Magedanz et al., 2015).

HFP steady state calculations were performed using CTF/TORT-TD with and without modeling of the fuel TCD. The same test case was simulated with CTF/TORT-TD/FRAPCON, where the fuel rods were modeled with the fuel performance code FRAPCON. HFP conditions were used in order to simulate a more realistic reactor environment where the spatial distributions of power and fuel temperature are important.

2.1. FRAPCON model

The geometry and composition of each fuel rod were obtained from the Purdue MOX benchmark (Kozlowski and Downar, 2007). Cross-sections for TORT-TD calculations were taken from the previous work of Magedanz et al. (2015). The cold, as-manufactured, fuel dimensions are given in Table 1. The same dimensions were used within the two coupled codes systems.

One MOX and one UO₂ fuel rod models were prepared for FRAPCON calculations. The Purdue MOX benchmark specification does not provide certain geometry information such as the plenum length and pellet dish size, which is required as an input for FRAPCON; therefore, values from available sample input files (Magedanz et al., 2015) were used. Both fuel rod types were burned for a total of 1000 days at a constant, axially-uniform power, which was calculated as the average-pin nominal power from the benchmark. Table 2 summarizes the input parameters used in FRAPCON for both fuel types. Table 3 shows the nodalization and Table 4 shows the characteristics of each fuel type.

2.2. CTF model

The CTF model, as shown in Fig. 2, consists of fifteen (15) fuel rods and one (1) control guide tube, all arranged in an array of twenty-five (25) sub-channels. There are three sub-channel geometry types – central sub-channel, side sub-channel, and corner sub-channel; and two inter-channel transverse connections types – with a half-gap width and with a full-gap width. Sub-channel

Table 11
CTF fuel rod models.

Fuel rod models	Fuel thermal conductivity model	Gap conductance
No TCD (IFRAP = 0)	MATPRO-11	CTF dynamic
TCD (IFRAP = 1)	Modified/NFI for UO ₂ or Duriez/NFI for MOX	CTF dynamic

Table 12
Fuel properties used in CTF calculations.

Fuel properties	Built-in UO ₂ properties
Clad properties	Build-in zirconium-dioxide properties
% Theoretical fuel density	93.35

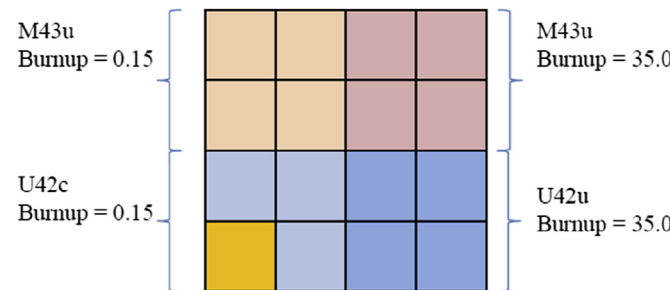


Fig. 3. TORT-TD assembly arrangement.

Table 13
TORT-TD model characteristics.

Number of energy groups	8
Number of delayed neutron precursors	6
Legendre scattering order	1
Quadrature type	Symmetric
Quadrature order	s_8

Table 14
TORT-TD axial nodalization.

Active core	Length [m]	3.6576
	Nodes	40 (equal size)
Lower reflector	Length [m]	0.3
	Nodes	5 (equal size)
Upper reflector	Length [m]	0.3
	Nodes	5 (equal size)

geometry characteristics and inter-channel transverse connection parameters are provided in Table 5 and Table 6, respectively. Modeling options were selected based on recommended and/or typical values for a PWR (provided in Table 7). The boundary conditions for coolant enthalpy, mass flow and outlet pressure were obtained from the Purdue MOX benchmark (provided in Table 8). Table 9 shows the radial and axial nodalization. Table 10 gives the spacer grid information used in the CTF calculations (Magedanz et al., 2015).

The CTF fuel rod model uses the dimensions shown in Table 1 with MATPRO-11 fresh UO₂ fuel properties for both UO₂ and MOX fuel rods. Selected fuel modeling options and the fuel properties

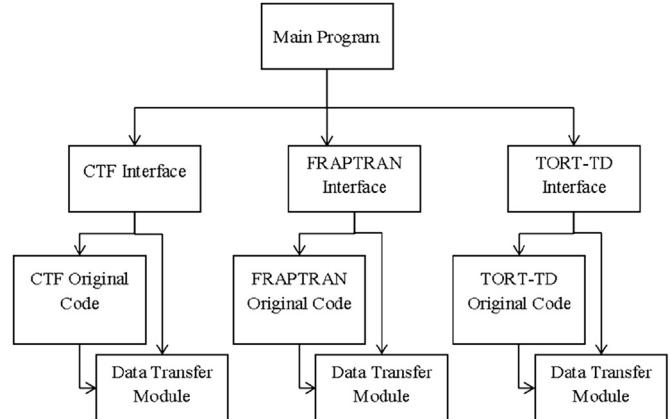


Fig. 4. Coupling interface structure.

used in CTF are provided in Table 11 and Table 12, respectively. The two fuel rod modeling options were:

- 1) The first option, also called “IFRAP = 0”, utilizes MATPRO-11 fuel thermal conductivity data, which is only a function of temperature for both UO₂ and MOX fuel rods. It also uses the UO₂ fuel properties for MOX fuel rods.
- 2) The second option, also called “IFRAP = 1”, utilizes the modified NFI fuel thermal conductivity model, for the UO₂ fuel rods and the modified Duriez/NFI fuel thermal conductivity model for the MOX fuel rods.

Both options were used along with the dynamic gap conductance model of CTF and were considered for steady state multi-channel analysis.

2.2.1. Burnup-dependent fuel thermal conductivity model

In the early versions of CTF, the fuel thermal conductivity was based on the MATPRO-11 material properties correlation from 1979 (Salko and Avramova, 2013), in which only a temperature dependence of the fuel thermal conductivity was assumed (Equation (1)) and the effects of the fuel burnup and the presence of burnable poisons (gadolinium concentration) were not considered. Moreover, the same temperature dependence was applied to both UO₂ and MOX fuels.

The thermal conductivity, k_{UO_2} , in CTF was calculated as (Salko and Avramova, 2013):

$$k_{UO_2} = \left[\max\left(0.0191, \frac{40.4}{(T - 273.15) + 464.0}\right) + 1.216 \times 10^{-4} e^{(1.867 \times 10^{-3} \times (T - 273.15))} \right] \times C, \quad (1)$$

where k_{UO_2} is the fuel thermal conductivity in W/m-K;

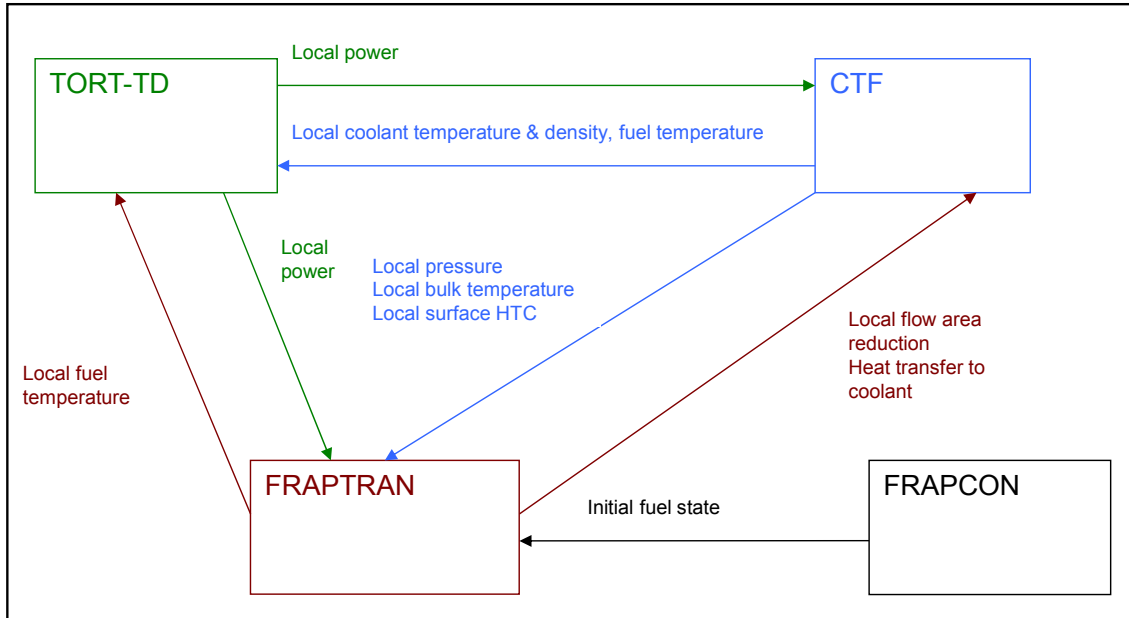


Fig. 5. Data transfer between CTF and FRAPTRAN with TORT-TD feedback.

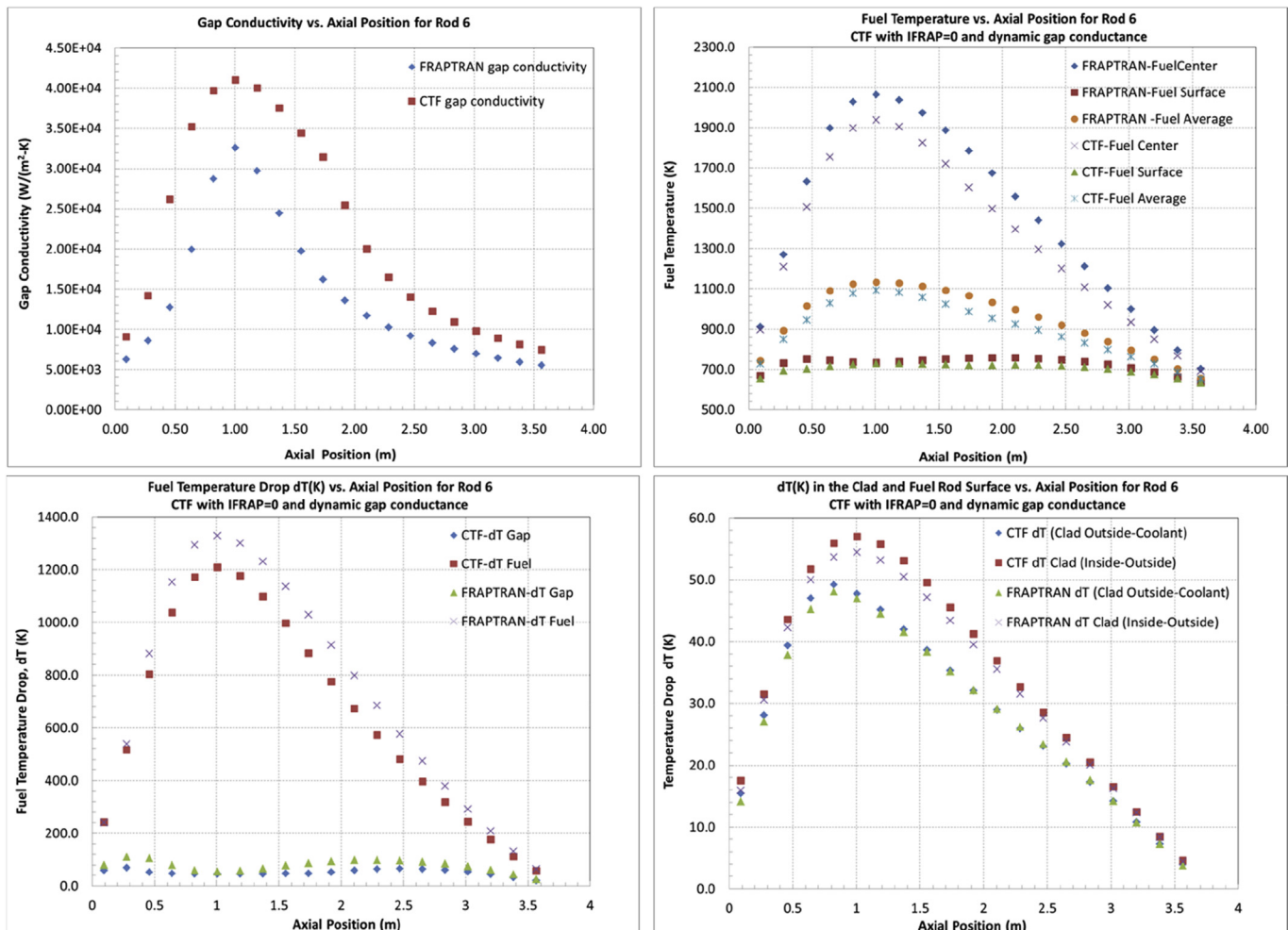


Fig. 6. CTF without TCD vs. FRAPTRAN Fuel Temperature Comparisons for Rod 6 (Low burnup MOX).

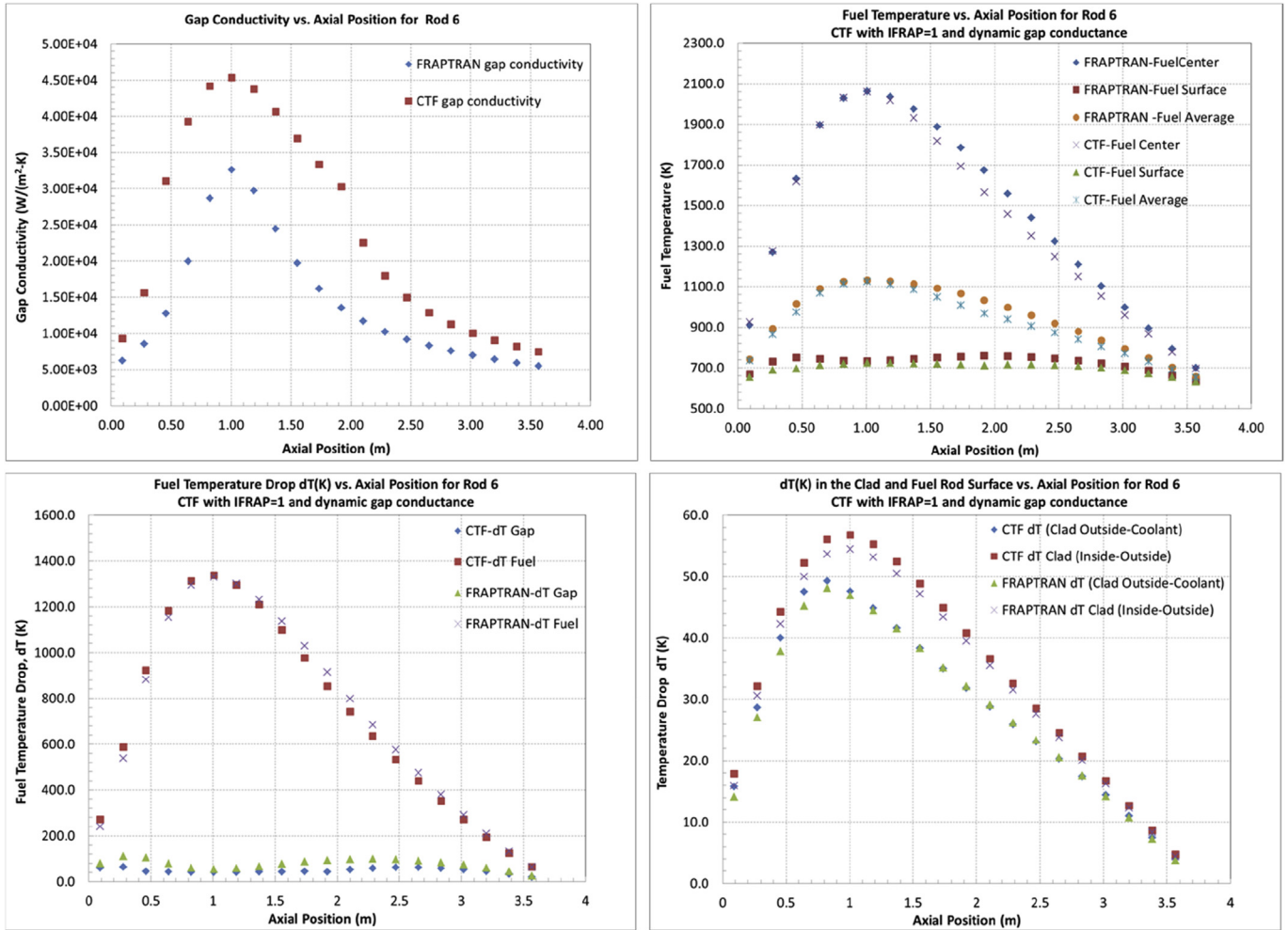


Fig. 7. CTF with TCD vs. FRAPTRAN Fuel Temperature Comparisons for Rod 6 (Low burnup MOX).

$$C = 100 \times \left(\frac{1 - \beta(1 - f_D)}{(1 - 0.05\beta)} \right); \quad (2)$$

$$\beta = 2.58 - 5.8 \times 10^{-4} \times (T - 273.15); \quad (3)$$

T is the temperature in K; and f_D is the dimensionless fuel theoretical density.

A literature survey was performed and the modified NFI fuel thermal conductivity model was chosen for implementation in CTF. The modified NFI model represents the fuel thermal conductivity as a function of burnup, temperature and gadolinium concentration, as shown in Equation (4) (Lusher and Geelhood, 2010):

$$k_{95} = \frac{1}{A + a.gad + BT + f(Bu) + (1 - 0.9e^{-0.04Bu})g(Bu)h(T)} + \frac{E}{T^2} e^{-F/T}, \quad (4)$$

where k_{95} is the thermal conductivity of UO₂ and UO₂-Gd₂O₃ fuel pellets for 95% dense fuel in W/m-K; T is the temperature in K; Bu is the burnup in GWd/MTU; gad is the weight fraction gadolinia; $f(Bu) = 0.00187 Bu$ accounts for the effect of fission

products in the crystal matrix (solution); $g(Bu) = 0.038.Bu^{0.28}$ accounts for the effect of irradiation defects; $h(T) = 1/(1 + 396 e^{-Q/T})$ is the temperature dependence of annealing on irradiation defects; $Q = 6380$ K; $A = 0.0452 \frac{m-K}{W}$; $a = 1.1599$ is a constant;

$$B = 2.46 \times 10^{-4} \frac{m-K}{W/K}; E = 3.9 \times 10^{-9} \frac{W-K}{m}; \text{ and } F = 16361 \text{ K}$$

The thermal conductivity model is adjusted for as fabricated fuel density using the Lucuta's recommendation for spherical-shaped pores (Lusher and Geelhood, 2010):

$$k_d = 1.0789 k_{95} \left(\frac{d}{[1 + 0.5(1 - d)]} \right), \quad (5)$$

where d is the density as a fraction of the theoretical density; k_{95} is the conductivity based on 95% theoretical density; k_d is the thermal conductivity adjusted for as fabricated fuel density; 1.0789 is the adjustment factor for conductivity at 100% theoretical density.

The Duriez/modified NFI model for MOX fuels was developed by combining the Duriez stoichiometry-dependent correlation and the modified NFI model. The Duriez correlation was derived from diffusivity measurements on unirradiated fuel pellets and the

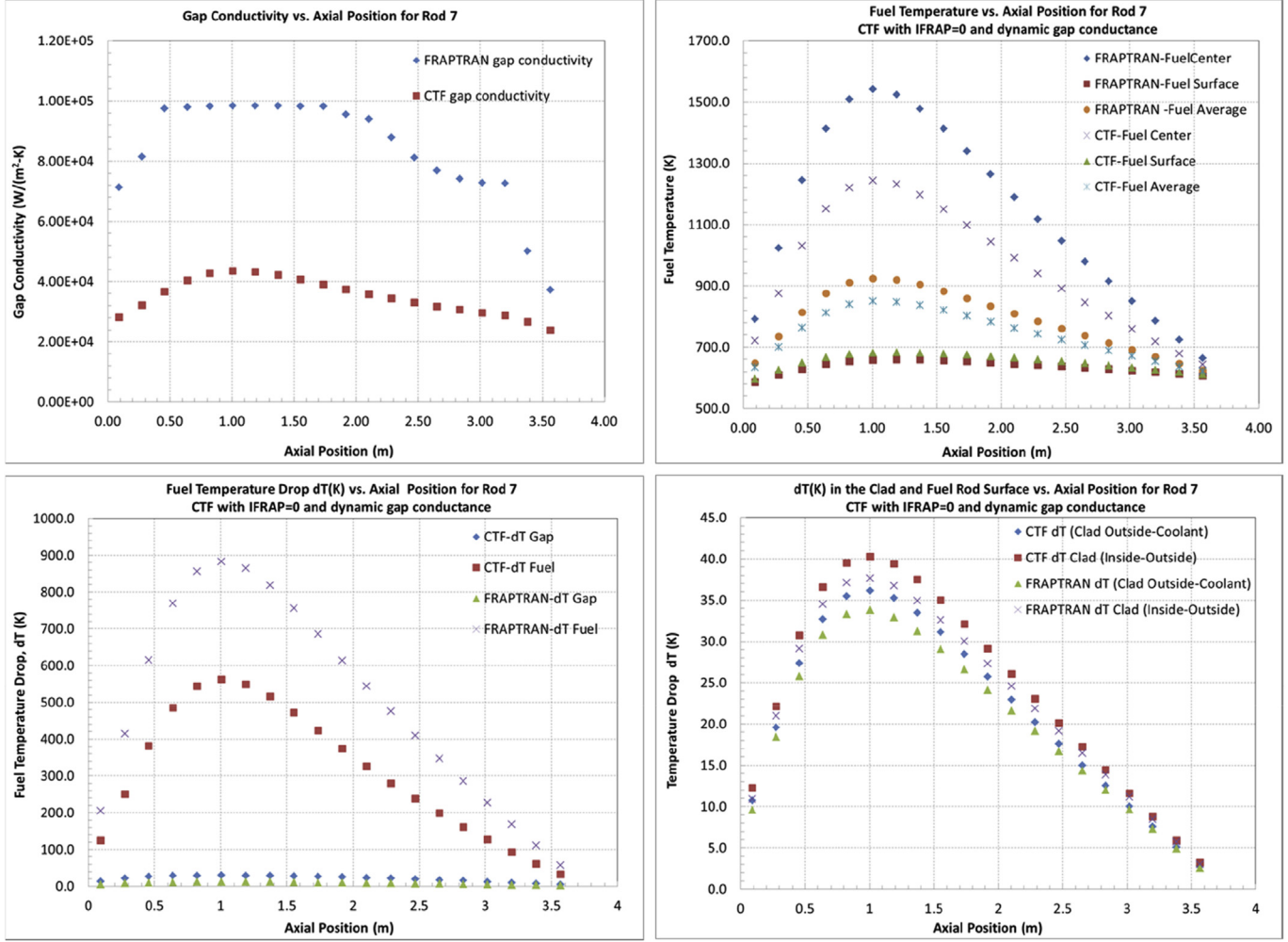


Fig. 8. CTF without TCD vs. FRAPTRAN Fuel Temperature Comparisons for Rod 7 (High burnup MOX).

modified NFI model included the burnup degradation effects. The Duriez thermal conductivity correlation has greater dependence of MOX, but only a minor dependence on plutonia content. The Duriez/modified NFI model is given as:

$$C_{mod} = 1.5 \times 10^9 \frac{W - K}{m}; D = 13520K;$$

$T, gad; Bu; f(Bu), g(Bu), h(T), Q, A$, and a are defined as in Equation

$$k_{95(MOX)} = \frac{1}{A(x) + a*gad + B(x)T + f(Bu) + (1 - 0.9 \exp(-0.04Bu))g(Bu)h(T)} + \frac{C_{mod}}{T^2} \exp\left(\frac{-D}{T}\right), \quad (6)$$

where $k_{95(MOX)}$ is the thermal conductivity of $(U, Pu)_O_2$ fuel at 95% theoretical density in $W/m \cdot ^\circ K$;

$$\begin{aligned} x &= 2.0 - \frac{O}{M} \text{ (i.e. oxygen - to - metal ratio); } A(x) \\ &= 2.8x + 0.035 \frac{m - K}{W}; B(x) = (2.86 - 7.15x) \times 10^{-4} \frac{m}{W}; \end{aligned}$$

(4).

2.2.2. Dynamic gap gas conductance model

The dynamic gap conductance model in CTF has the following three sub-components: (a) conductance due to thermal radiation; (b) conduction in the fill gas; and (c) conduction due to physical contact between the fuel pellet and the cladding. The reader should be aware that the model does not account for the effects of burnup. A burnup-dependent gas gap conductance model is currently being developed and implemented in CTF; in addition, the model will

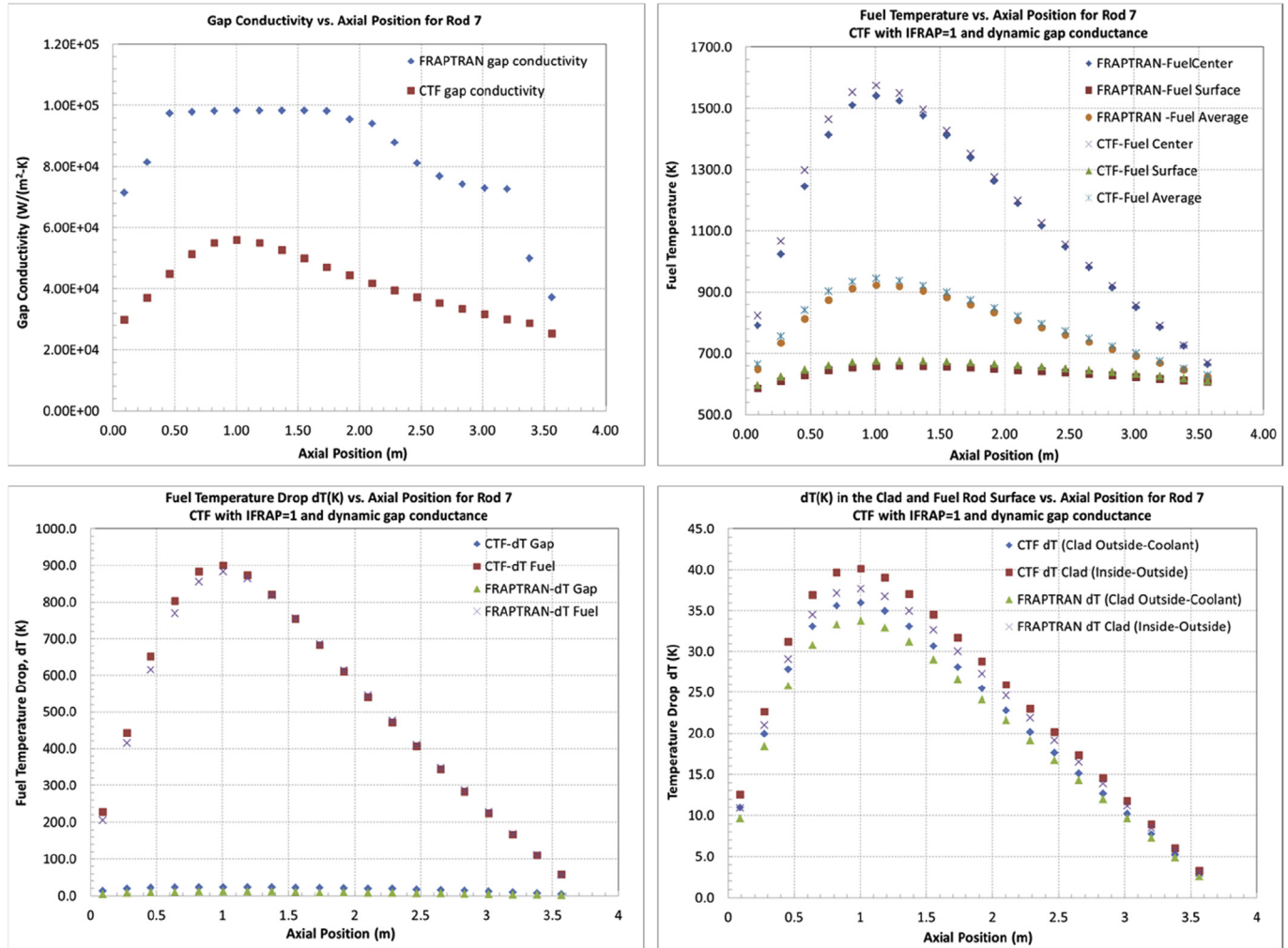


Fig. 9. CTF with TCD vs. FRAPTRAN Fuel Temperature Comparisons for Rod 7 (High burnup MOX).

take in consideration the power history and the instantaneous power changes.

Currently, the gap is assumed axisymmetric in the calculations and the gas gap conductance is given as:

$$h_{gap} = h_{rad} + h_{gas} + h_{solid}, \quad (7)$$

where h_{gap} is the total gap conductance, W/m²-K; h_{rad} is the conductance due to radiation, W/m²-K; h_{gas} is the conductance through gas, W/m²-K; and h_{solid} is the contact conductance, W/m²-K.

The radiant heat flux is calculated from the following Stefan-Boltzmann equation (Salko and Avramova, 2013):

$$q_r'' = \sigma_{SB} \frac{T_f^4 - T_c^4}{\frac{1}{\epsilon_f} + \frac{A_{fo}}{A_{co}} \left(\frac{1}{\epsilon_c - 1} \right)}, \quad (8)$$

where $\sigma_{SB} = 5.670373 \times 10^{-8} \frac{W}{m^2 \cdot K^4}$ is the Stefan-Boltzmann constant; T_f is the fuel surface temperature in K; T_c is the cladding surface temperature in K; ϵ_f is the fuel surface emissivity (constant value); A_{fo} is the fuel surface area in m²; A_{co} is the cladding

surface area in m²; ϵ_c is the cladding surface emissivity (constant value); and q_r'' is the radiant heat flux leaving the fuel surface in W/m².

The gap conductance due to the radiant heat transfer is expressed as a ratio of the gap radiant heat flux, q_r'' , to the temperature rise across the fuel to cladding gap (Salko and Avramova, 2013):

$$h_{rad} = \frac{q_r''}{T_f - T_c}, \quad (9)$$

where h_{rad} is the conductance due to radiation in W/m²-K; T_f is the fuel surface temperature in K; and T_c is the cladding surface temperature in K.

CTF assumes that the convective heat transfer caused by the fill gas is negligible due to the very thin gap structure between the fuel pellet and cladding. The heat transfer by conduction through the fill gas will exist whether the gap is open or closed due to the fuel expansion; however, the calculation of the heat conduction in the fill gas in a closed gap will be slightly different than that in an open gap. The CTF fuel deformation module first calculates the physical gap thickness t_g and the jump distances g_1 and g_2 (g_1 and g_2 are the

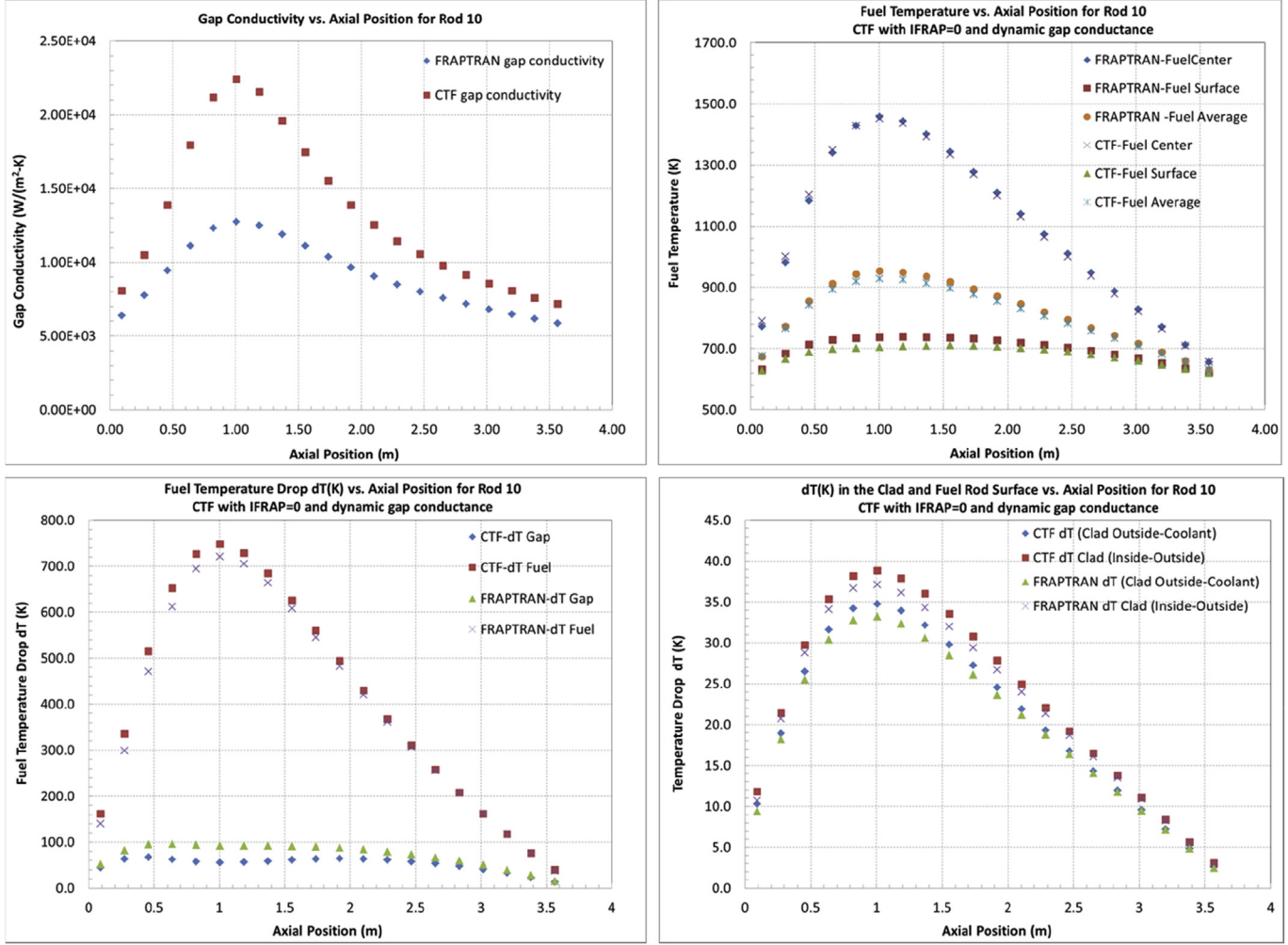


Fig. 10. CTF without TCD vs. FRAPTRAN Fuel Temperature Comparisons for Rod 10 (Low burnup UO₂).

fuel pellet temperature jump distance and the cladding temperature jump distance, respectively).

Then, it compares the physical gap thickness to a combination of surface roughness of fuel and clad and dimensionless modification factor. The dimensionless modification factor accounts for interface pressure, which determines whether the gap is closed or open. The gap is assumed to be closed when the calculated gap thickness is less than 3.6 times the sum of the surface roughness as shown in Equation (10):

$$t_g < 3.6 * (R_1 + R_2), \quad (10)$$

where t_g is the gas gap width in m; R_1 is the mean outer surface roughness of the fuel pellet in m; R_2 is the mean inside surface roughness of the cladding in m.

For both cases, the gas heat conduction is defined as the gas mixture conductivity (k_{gas} , W/m-K) divided by the total effective gap thickness (h_{gas} , m):

$$h_{gas} = \frac{k_{gas}}{\delta_{gas}} \quad (11)$$

The CTF model incorporates the discontinuity while adding the temperature jump distances (g_1 and g_2) into the gas conduction equation given in Equation (11) that is used for the open gap calculation:

$$h_{gas} = \frac{k_{gas}}{[t_g + 1.8 * (g_1 + g_2)]}, \quad (12)$$

where t_g is the gas gap width in m; g_1 is the fuel pellet temperature jump distance in m; and g_2 is the cladding temperature jump distance in m. The term “discontinuity” is used in thermal-mechanical calculations for the fill gas conductance in the very thin gap structure between the fuel pellet and the cladding. The discontinuity in the gap temperature near to the fuel pellet surface and clad occurs due to the incomplete thermal mixing of the gas molecules in this localized region; thus temperature jump distances in the gap gas conductance equations are added.

After determining the existence of closed gap condition, CTF uses a slightly different formula (Equation (13)) to calculate the gas fill gap conductance component. The model used for calculating gap fill heat conduction was based on a linear regression analysis of Ross-Stoute data by Lanning and Hann (Salko and Avramova, 2013;

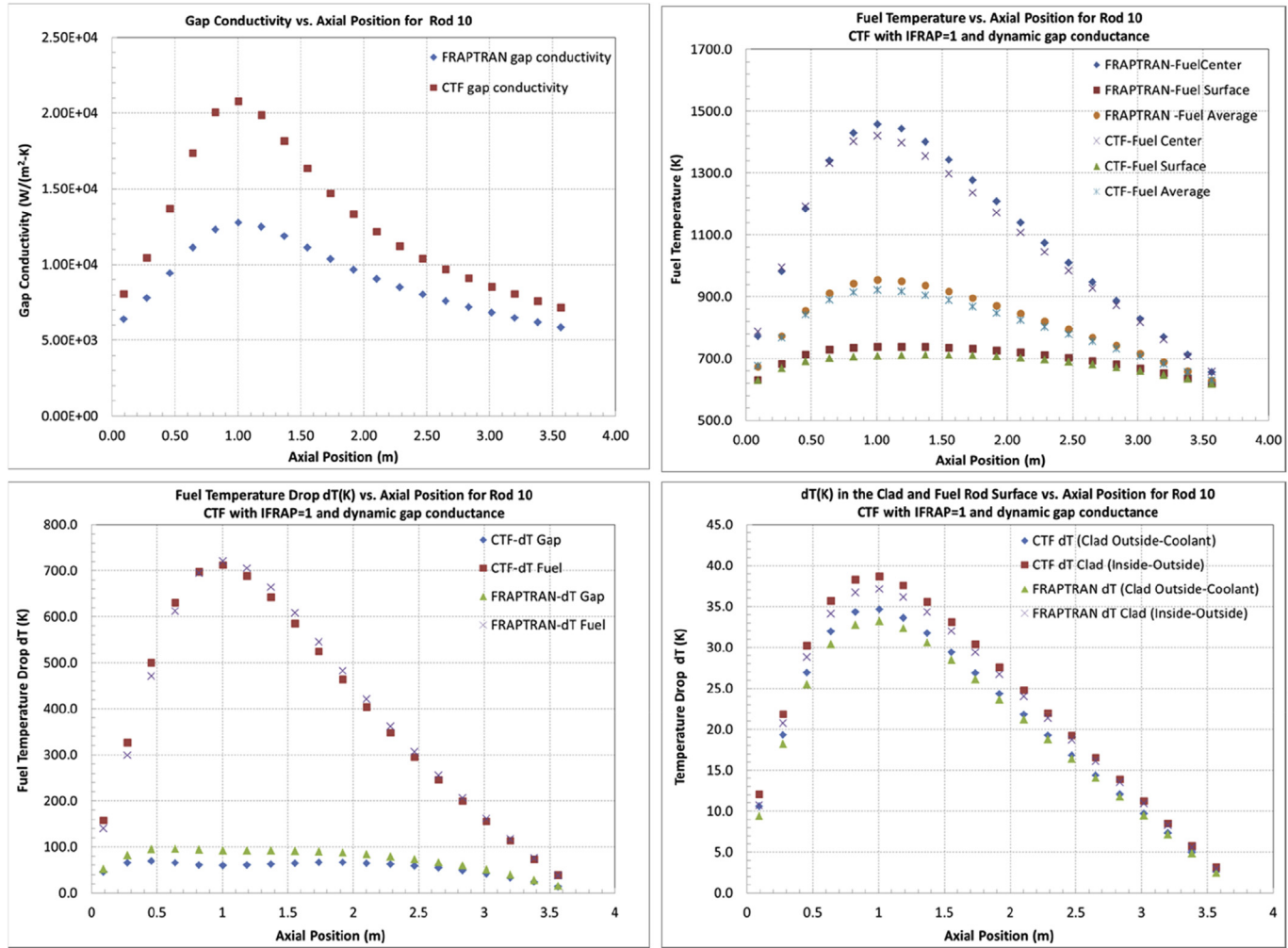


Fig. 11. CTF with TCD vs. FRAPTRAN Fuel Temperature Comparisons for Rod 10 (Low burnup UO₂).

Lanning and Hann, 1975):

$$h_{gas} = \frac{k_{gas}}{[1.8 [C(R_1 + R_2) + (g_1 + g_2)] - 1.2 \times 10^{-6}]}, \quad (13)$$

where $C = 2.0e^{-0.00125P_{int}}$ is a dimensionless modification factor accounting for interface pressure; P_{int} is the fuel-cladding interfacial pressure in kg/cm²; R_1 is the mean outer surface roughness of the fuel pellet in m; and R_2 is the mean inside surface roughness of the cladding in m.

The thermal conductivity of the gas mixture is calculated by considering all of the individual gas conductivities and their molecular weights and fractions. In addition to the thermal conductivity, the temperature jump distance is also calculated based on the Lloyd model (Salko and Avramova, 2013; Lanning and Hann, 1975; Lloyd et al. (1973), 1973). The gap temperature jump distance is given as a function of the fill gas thermal conductivity, the mean gas gap temperature, the fill gas pressure and the molecular fraction of each gas molecules in the gap.

The solid conduction term will be calculated when the deformation model determines that calculated gap thickness is small

enough for a contact to occur. Otherwise, the term will be zero, if the contact condition is not met. The Mikic/Todreas model (Salko and Avramova, 2013; Lanning and Hann, 1975; Todreas and Jacobs, 1973) is used for the heat transfer coefficient calculation:

$$h_{solid} = \frac{0.4166 * k_m}{\sqrt{R_f^2 + R_c^2}} \left(\frac{P_{int}}{H_Z} \right)^n \left(\frac{R_f}{\lambda_f} \right), \quad (14)$$

where h_{solid} is the contact conductance in W/m²-K; $\left(\frac{P_{int}}{H_Z} \right)^n$ is the dimensionless ratio of the interface pressure to the Meyer hardness; $\left(\frac{R_f}{\lambda_f} \right)$ is the dimensionless ratio of the mean fuel surface roughness and wavelength; R_f is the mean fuel roughness in m; R_c is the mean cladding roughness in m; $k_m = \frac{2k_f k_c}{k_f + k_c}$ is the geometric mean conductivity at the interface in W/m-K; and n is based on the value of the non-dimensionalized interface pressure.

For $P_{int}/H_Z < 0.0001$, n is set to 0.5. For values of P_{int}/H_Z between 0.001 and 0.01, the entire expression, $(P_{int}/H_Z)^n$, is 0.01. For values of

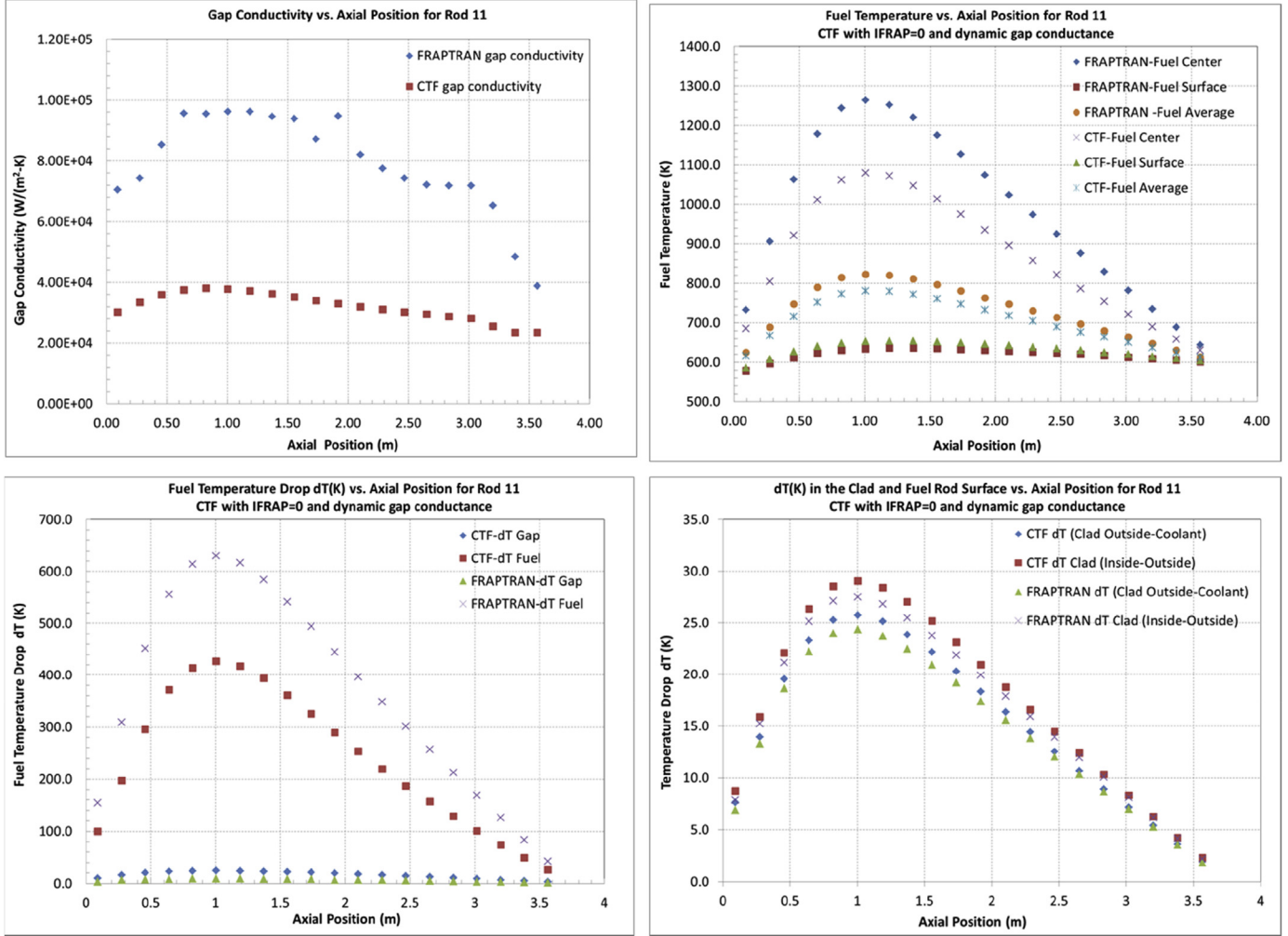


Fig. 12. CTF without vs. FRAPTRAN Fuel Temperature Comparisons for Rod 11 (High burnup UO₂).

$(P_{int}/Hz) > 0.01$, n is set to 1.0. The ratio of the fuel surface roughness to wave length is estimated by Equation (15), where R_f is the mean fuel roughness in meters (Salko and Avramova, 2013):

$$\left(\frac{R_f}{\lambda_f}\right) = \exp \left[0.5285 * \ln \left(3.937 * 10^{-7} * R_f \right) - 5.738 \right] \quad (15)$$

2.3. TORT-TD model

TORT-TD performs three-dimensional (3D) steady state and transient neutron-kinetics calculations, based on the discrete ordinates (S_N) method. The TORT-TD model for this problem uses eight neutron energy groups and S8 angular discretization with symmetric, equal angular mesh sizes. The model, shown in Fig. 3, has sixteen (16) nodes on the x-y plane – one for each fuel rod or a guide tube. It has forty (40) axial nodes in the active core region. In addition, a reflector region is modeled above and below the active core (Magedanz et al., 2015). Table 13 and Table 14 provide the TORT-TD model properties and the TORT-TD axial nodalization,

respectively. TORT-TD pin-cell arrangement is shown in Fig. 3 – the x-y plane is divided into four (4) regions and each region has four (4) fuel pins. The regions consists of a low burnup MOX fuel, a high burnup MOX fuel, a low burnup UO₂ fuel, and a high burnup UO₂ fuel. The low burnup UO₂ region has one (1) control rod guide tube with three (3) UO₂ pins surrounding it.

The cross section libraries used were generated by the HELIOS code and each region pin cell (UO₂, MOX, control guide tube and reflector) is modeled separately. The power input to TORT-TD is determined by the pin-average nominal power for fifteen (15) fuel pins for the HFP steady state conditions. The control rod is fully withdrawn.

2.4. CTF/TORT-TD/FRAPCON coupled system

CTF, FRAPCON and TORT-TD have been previously integrated into a single code by using serial integration techniques with some parallelism for the FRAPCON calculations. The detailed description of the coupling structure, code interfaces, and information exchanged is given in (Magedanz et al., 2015). This study extends the previous work by incorporating the new thermal conductivity

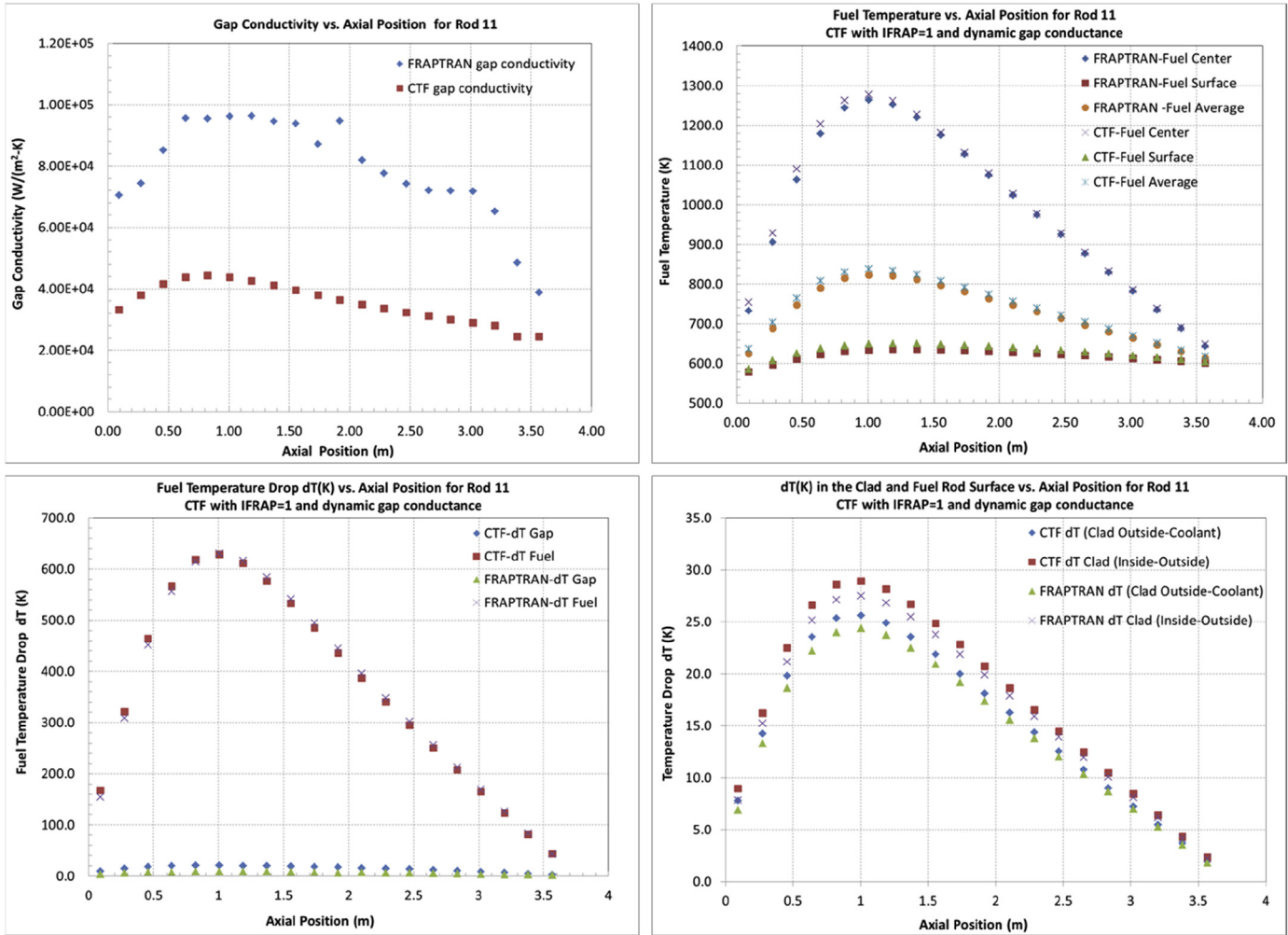


Fig. 13. CTF with TCD vs. FRAPTRAN Fuel Temperature Comparisons for Rod 11 (High burnup UO₂).

model in the CTF calculations. The source code modifications occurred within CTF modules have also been incorporated in the coupled CTF/TORT-TD/FRAPCON code. The updated version of the coupled code was recompiled to analyze the impact of the fuel TCD model in CTF for fully coupled steady state and transient calculations. Therefore, the coupling interface and information flow between codes is briefly summarized below.

The layer abstraction technique was used to separate the main program and the involved single physics codes from each other within an object-oriented programming structure (Magedanz et al., 2015). Utilizing this method, all variables within each single physics code were separated and encapsulated from other program access. All communications between codes occurred via “interface” methods. The top level system diagram of the coupling structure is given in Fig. 4. It shows that each interface has a data transfer module sharing its data with the main program and other interfaces. As previously discussed, the coupled code system CTF/TORT-TD/FRAPTRAN uses FRAPCON-generated data for steady state calculations. In other words, the CTF/TORT-TD/FRAPCON is used to generate reference solutions for steady state conditions while the CTF/TORT-TD/FRAPTRAN does the same for transient scenarios.

Data transfer between CTF and FRAPCON with TORT-TD

feedback is given in Fig. 5. Flow area and wetter perimeter changes due to total heating in the coolant channels (which are tightly coupled to fuel rods with changing fuel rod area and perimeter parameter at each time interval) are transferred from FRAPCON to CTF. From the CTF calculations, where the cladding temperature is used to determine flow regimes, the friction factor and the heat transfer coefficients are transferred back to FRAPCON calculations. The fuel rods can be modeled by either CTF or FRAPCON and the fuel temperature is extracted from the code that models the fuel rod. TORT-TD power distribution can be transferred to both CTF and FRAPCON calculations.

As described in the previous sections CTF has its own fuel rod model, which has been improved by implementing the same TCD as implemented in FRAPCON. The objective of this paper is to compare the results obtained with the improved CTF fuel rod model in coupled (multi-physics) calculations to reference predictions of CTF/TORT-TD/FRAPCON, which are produced using the fuel rod model of FRAPCON.

3. Steady state fuel temperature comparisons

In both CTF/TORT-TD simulations with and without modeling of the fuel TCD, the dynamic gas gap conductance model (Equations

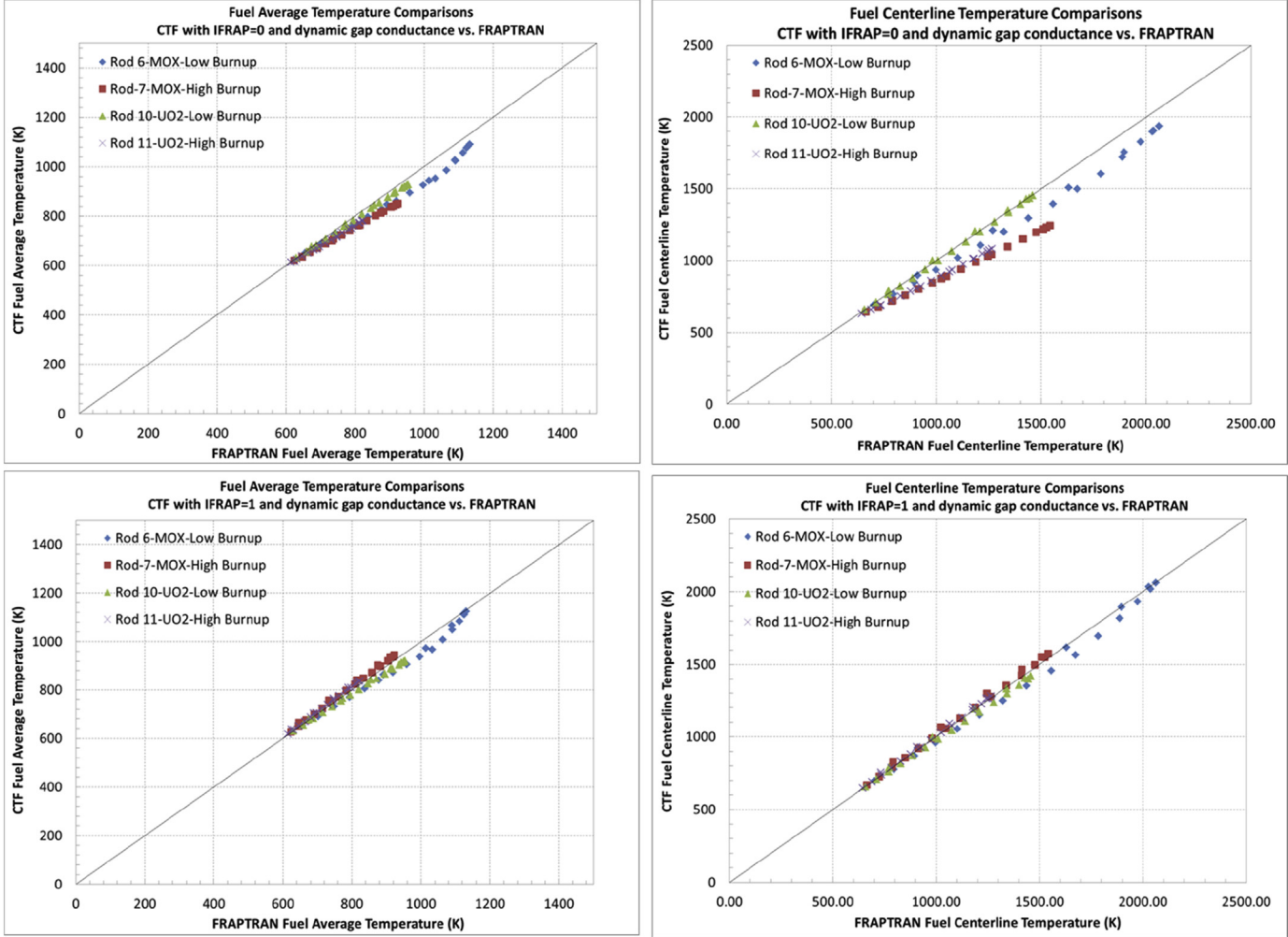


Fig. 14. CTF vs. FRAPTRAN Fuel Temperature Comparisons.

(7)–(15)) was used. Figs. 6–14 compare fuel temperature predictions from the two models to the CTF/TORT-TD/FRAPCON results for rods 6, 7, 10 and 11, respectively. Fig. 15 shows the radial power profile used for each fuel rod type.

As seen from the gap conductance plots in Figs. 6–14, CTF and FRAPCON calculate different gap conductance values. The reason for the observed differences is that CTF does not model the fuel thermal-mechanical effects such as the fuel swelling and densification, which will have an impact on the physical gap. In addition, FRAPCON updates the gap gas compositions during burnup, but CTF does not. Thus, CTF over-predicted the gap conductance of the low burnup fuel rods, Rod 6 (Fig. 6 and Fig. 7) and Rod 10 (Fig. 10 and Fig. 11), as compared to FRAPCON. The reason for this is the lack of a fuel densification modeling in the thermal-hydraulics code CTF, while the larger physical gap predicted by the FRAPCON densification model resulted in a lower gap conductance. In contrast, CTF shows an under-prediction of the gap conductance of high burnup fuel rods – Rod 7 (Fig. 8 and Fig. 9) and Rod 11 (Fig. 12 and Fig. 13). The reason for this is the lack of a fuel swelling model in CTF, while the smaller physical gap predicted by the FRAPCON fuel swelling model resulted in a higher gap conductance. For low burnup fuel rods CTF predicted $1 \times 10^4 \text{ W/m}^2\text{--}^\circ\text{K}$ higher gap conductance value than FRAPCON, while for high burnup rods FRAPCON predicted $6 \times 10^4 \text{ W/m}^2\text{--}^\circ\text{K}$ higher gap conductance value. Although CTF and

FRAPCON gave different gap conductance, the temperature drop across the gap between the two codes was within 20 K difference. Fig. 14 compares CTF and FRAPCON predictions of the fuel centerline and fuel average temperatures. As expected, CTF without burnup-dependent fuel conductivity underpredicts the fuel centerline temperature. For better illustration, Fig. 15 shows the in-pellet radial power profiles used in CTF and FRAPCON.

Gap conductance plots for fresh fuels in Figs. 6, 7, 10 and 11 also show that the peak in the gap conductance was observed at the peak power location. This is due to the expansion of the fuel pellet at high temperatures. High power levels result in higher temperatures causing the fuel pellet to expand more.

Table 15 shows comparisons of the effective neutron multiplication factor, k_{eff} , as predicted by CTF/TORT-TD with and without fuel TCD modeling, and by CTF/TORT-TD/FRAPCON. The agreement with the reference CTF/TORT-TD/FRAPCON calculation was significantly improved when fuel TCD was taken into account in CTF/TORT-TD simulations: the difference in the predicted reactivity decreased from 117 pcm to -5 pcm. These results show that disregarding the changes in the fuel properties with burnup would lead to under-prediction of the fuel (Doppler) temperature, and thus over-prediction of the effective neutron multiplication.

Table 16 and Table 17 summarize the statistical analysis performed with the two fuel thermal conductivity options. The

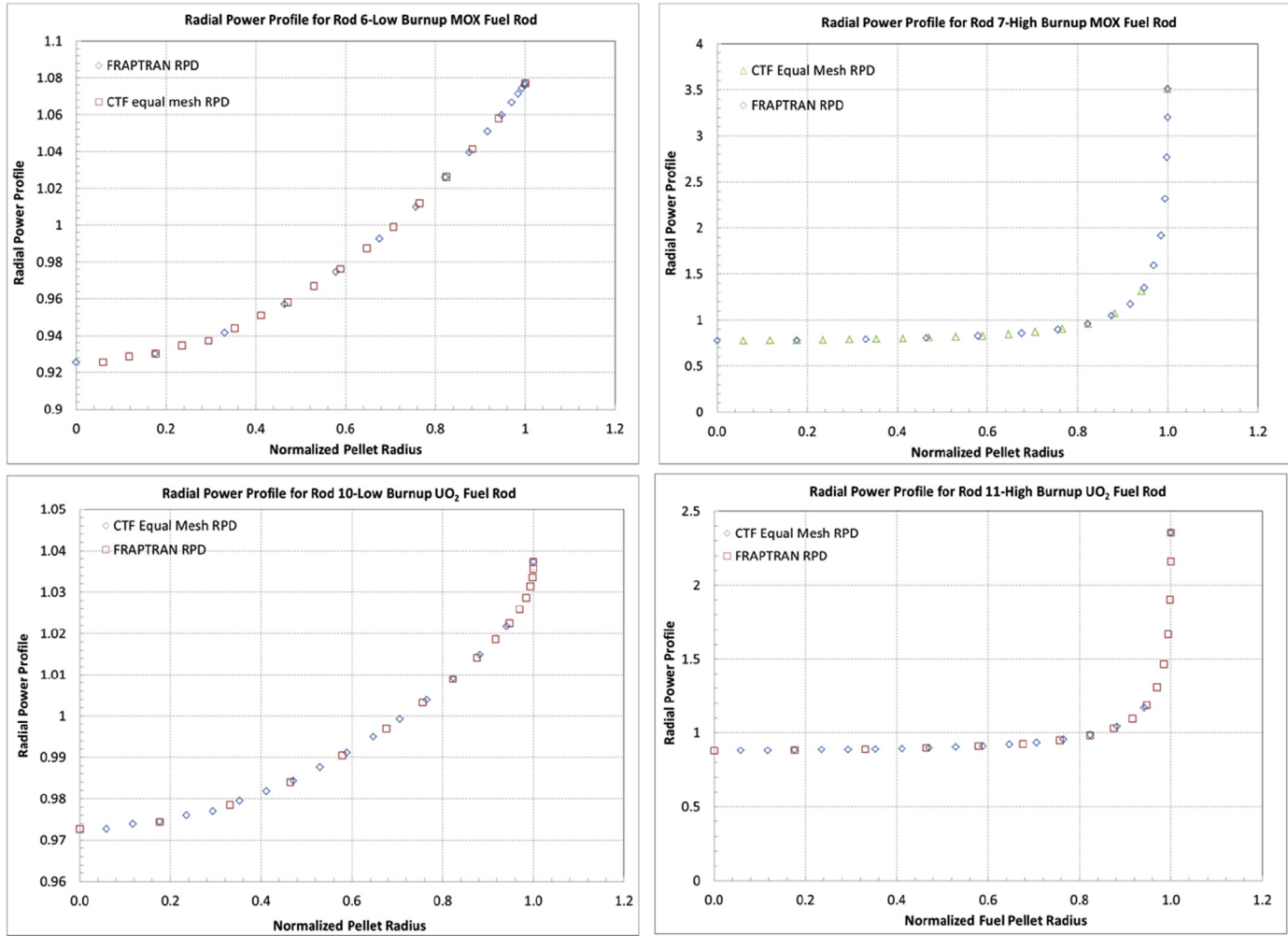


Fig. 15. CTF vs. FRAPTRAN Radial Power Distribution.

Table 15
Neutron multiplication factor results.

	CTF/TORT-TD/ FRAPCON	CTF/TORT-TD without TCD	CTF/TORT-TD with TCD
K _{eff} (unrodded)	1.10544	1.10661	1.10539
Reactivity difference [pcm]	—	117	-5

Table 16
Statistics for CTF without fuel thermal conductivity degradation modeling.

Rod number	Type	Burnup	T _{center} Mean	T _{center} STD	T _{average} Mean	T _{average} STD
6	MOX	Low	0.9299	0.0261	0.9504	0.0189
7	MOX	High	0.8542	0.0469	0.9494	0.0225
10	UO ₂	Low	0.9982	0.0098	0.9850	0.0081
11	UO ₂	High	0.8907	0.0363	0.9664	0.0146
All rods			0.9182	0.0626	0.9628	0.0223

enhanced accuracy of the new model is clearly demonstrated. CTF/TORT-TD with the thermal conductivity degradation model resulted in a lower standard deviation in centerline temperature: 0.0247 versus 0.0626; and in a higher mean value: 0.9957 versus 0.9182.

Table 17
Statistics for CTF with fuel thermal conductivity degradation modeling.

Rod number	Type	Burnup	T _{center} Mean	T _{center} STD	T _{average} Mean	T _{average} STD
6	MOX	Low	0.9726	0.0254	0.9685	0.0183
7	MOX	High	1.0171	0.0129	1.0193	0.0075
10	UO ₂	Low	0.9839	0.0157	0.9805	0.0116
11	UO ₂	High	1.0093	0.0086	1.0142	0.0053
All rods			0.9957	0.0247	0.9956	0.0246

The uncertainty in the temperature calculations were reduced and the CTF/TORT-TD prediction capabilities were significantly improved.

4. Conclusions

Fuel temperature (Doppler) feedback modeling in the coupled sub-channel thermal-hydraulic/time-dependent neutron transport codes system CTF/TORT-TD was improved by modeling the burnup dependence of the fuel thermal conductivity. It was demonstrated by comparisons with reference CTF/TORT-TD/FRAPCON solutions that the improved CTF/TORT-TD can be seen as a high fidelity multi-physics tool which provides accurate and efficient calculations for practical reactor core design and safety analysis.

Additionally, it was confirmed that using a constant value of the gas gap conductance in coupled thermal-hydraulics/neutronics calculations will significantly reduce their accuracy. Therefore, it is recommended to use the simplified dynamic gap conductance model in CTF. In this regard, a new improved gas gap conductance model is under implementation in the stand-alone and coupled CTF. The model will take into account the changes in the gap dimensions and gas mixture composition with burnup. The new CTF dynamic gap conductance model will utilize tabulated data and correlations based on reference high-fidelity high-resolution fuel thermal-mechanical simulations accomplished with a reliable fission gas release modeling. The new CTF capability will feature a full three-dimensional representation.

References

Geelhood, K.J., Luscher, W.G., Beyer, C.E., 2010. FRAPCON-3.4: a Computer Code for

- the Calculation of Steady-state, Thermal Mechanical Behavior of Oxide Fuel Rods for High Burnup, NUREG/CR-7022, PNNL-19418, vol. 1, vol. 1. Pacific Northwest National Laboratory, Richland, Washington.
- Geelhood, K.J., Luscher, W.G., Beyer, C.E., 2010. FRAPTRAN 1.4: a Computer Code for the Transient Analysis of Oxide Fuel Rods, NUREG/CR-7023. PNNL-19400, vol. 1, vol. 1. Pacific Northwest National Laboratory, Richland, Washington.
- Geelhood, K.J., Luscher, W.G., Beyer, C.E., 2010. FRAPCON-3.4: Integral Assessment, NUREG/CR-7022. PNNL-19418, vol. 2, vol. 2. Pacific Northwest National Laboratory, Richland, Washington.
- Kozlowski, T., Downar, T., 2007. PWR MOX/UO₂ Core Transient Benchmark: Final Report. NEA/NSC/DOC (2006)20. Purdue University.
- Lanning, D.D., Hann, C.R., 1975. Review of Methods Applicable to the Calculation of Gap Conductance in Zircaloy-clad UO₂ Fuel Rods, Technical Report BNWL-1894. Pacific Northwest Laboratory.
- Lloyd, W.R. et al. (1973). Heat Transfer in Multicomponent Monatomic Gases in the Low, Intermediate, and High Pressure Regime, in: Nuclear Thermionics Conference.
- Lusher, W.G., Geelhood, K.J., 2010. Material Property Correlations: Comparisons between FRAPCON-3.4, FRAPTRAN 1.4, and MATPRO, NUREG/CR-7024, PNNL-19417. Pacific Northwest National Laboratory, Richland, Washington.
- Magedanz, J., Avramova, M., Perin, Y., Velkov, K., 2015. "High-Fidelity Multi-physics System TORT-TD/CTF/FRAPTRAN for Light Water Reactor Analysis", Annals of Nuclear Energy, Special Issue on Multi-physics Modelling of LWR Static and Transient Behavior (Invited paper).
- Salko, R., Avramova, M., 2013. CTF Theory Manual, RDFMG/MNE/PSU. Penn State University, University Park, PA.
- Todreas, N., Jacobs, G., 1973. Thermal contact conductance of reactor fuel elements. Nucl. Sci. Eng. 50, 283.
- Yilmaz, M.O., 2014. Development of Burnup Dependent Fuel Rod Model in COBRA-TF, PhD Thesis in Nuclear Engineering. The Pennsylvania State University, University Park, PA.